Spatial Decomposition-Based Fault Detection Framework for Parabolic-Distributed Parameter Processes

Yun Feng, Yaonan Wang, Bing-Chuan Wang, and Han-Xiong Li, *Fellow, IEEE*

***Abstract*—Fault detection for distributed parameter processes (heat processes, fluid processes, etc.) is vital for safe and efficient operation. On one hand, the existing data-driven methods neglect the evolution dynamics of the processes and cannot guarantee that they work for highly dynamic or transient processes; on the other hand, model-based methods reported so far are mostly based on the backstepping technique, which does not possess enough redundancy for fault detection since only the boundary measurement is considered. Motivated by these considerations, we intend to investigate the robust fault detection problem for distributed parameter processes in a model-based perspective covering both boundary and in-domain measurement cases. A real-time fault detection filter (FDF) is presented, which gets rid of a large amount of data collection and offline training procedures. Rigorous theoretic analysis is presented for guiding the parameters selection and threshold computation. A time-varying threshold is designed such that the false alarm in the transient stage can be avoided. Successful application results on a hot strip mill cooling system demonstrate the potential for real industrial applications.**

***Index Terms*—Distributed parameter process, fault detection, partial differential equation (PDE) observer.**

I. INTRODUCTION

DISTRIBUTED parameter processes widely exist in industrial applications, for example, transport-reaction processes [1], snap curing processes [2]–[4], and battery thermal processes [5]–[7]. Generally, these processes can all be described by partial differential equations (PDEs) mathematically, which possess the spatial–temporal dynamics [8]–[12]. With the rapidly increasing demand for the high-production quality with economic operations for these industrial processes, the requirement of system safety is a critical issue that needs to be addressed. Faults hidden in these processes may cause system failure or even permanent damage if they are not discovered in time. For example, the distributed thermal fault in lithium-ion (Li-ion) batteries [5], [13] can lead to battery degradation, failure, and even thermal runaway. The in-domain actuator faults of diffusion-reaction processes [1], [14] that widely exist in chemical processes can cause severe effects. Despite the fact that advanced control design [15], [16] for distributed parameter systems (DPSs) (including sampled-data [17], [18] and fuzzy control [19]) were well studied in recent years, works reported on fault diagnosis for distributed parameter processes are relatively rare so far.

On one hand, for decades, the fault detection and fault-tolerant control for technical processes that are modeled by ordinary differential equations (ODEs) have been investigated sufficiently, from both model-based [20]–[22] and data-driven [23] perspectives; on the other hand, research focusing on the fault diagnosis of PDEs is relatively rare. Similarly, these works can be roughly separated into these two subcategories.

In terms of the data-driven fault detection for distributed parameter processes, some works have been reported recently (see [24]–[27] for reference). For example, by using the Galerkin method, a data-driven process monitoring approach for parabolic DPS was discussed [24]. A novel data-driven method was proposed for fault detection and localization of parabolic DPSs [25]. However, these methods either used modal approximation [24] which induces *observation spillover* or neglected the evolution dynamics of the processes [25], [27] and cannot guarantee work for highly dynamic or transient processes.

As for the existing model-based fault detection methods, they can be further divided into two subcategories: 1) the so-called "early-lumping" [28] approach that reduces the PDE into several approximated ODEs in the first place and then analyzes the ODE model (representative works can be referred to [1], [14], and [29]). The other was the so-called "late-lumping" approach [30], [31] which directly investigates the PDE system without approximation. Research belong to this category is mainly based on the backstepping

Manuscript received October 1, 2020; revised December 10, 2020; accepted January 3, 2021. This work was supported in part by the Applied Basic Research Fund of Guangdong Province under Grant 2019A1515011963; in part by the General Research Fund Project from Research Grant Council of Hong Kong, under Grant CityU: 11210719; in part by the National Nature Science Foundation (NSFC) under Grant 61733004; and in part by the Science and Technology Project of Hunan Province under Grant 2018GK2022 and Grant 2018JJ3079. This article was recommended by Associate Editor B. Jiang. *(Corresponding author: Yaonan Wang.)*

Yun Feng and Yaonan Wang are with the College of Electrical and Information Engineering, Hunan University, Changsha 410082, China, and also with the National Engineering Laboratory for Robot Visual Perception and Control Technology, Hunan University, Changsha 410082, China (e-mail: fyrobot@hnu.edu.cn; yaonan@hnu.edu.cn).

Bing-Chuan Wang is with the School of Automation, Central South University, Changsha 410083, China (e-mail: wangbingchuancityu@gmail.com).

Han-Xiong Li is with the Department of Systems Engineering and Engineering Management, City University of Hong Kong, Hong Kong (e-mail: mehxli@cityu.edu.hk).

Color versions of one or more figures in this article are available at https://doi.org/10.1109/TCYB.2021.3049453.

Digital Object Identifier 10.1109/TCYB.2021.3049453

design techniques [32] (see [13] and [33]). "Early-lumping"-based approaches have been criticized for the *observation spillover* induced by the modal approximation used. Moreover, for the backstepping-based fault detection methods, the redundancy cannot be guaranteed for certain applications since only boundary measurement is used. Hence, a unified framework for fault detection, which can be applied to either the boundary and in-domain sensor, is still missing.

Considering the above facts, we are devoted to the study of a methodology framework for robust fault detection of distributed parameter processes from a model-based perspective while covering both boundary and in-domain measurement cases. To be more specific, a fault detection filter (FDF) is first constructed to generate signals by mimicking the FDF design of lumped parameter systems (LPSs) [20]. Furthermore, the residual evaluation scheme and threshold computation procedure are conducted in a similar manner.

The remainder of this article can be summarized as follows. In Section II, the detailed problem statement is introduced. The methodology framework is illustrated in Section III. The Luenberger-type PDE observer and FDF design are presented in Sections IV and V, respectively. Illustrative demonstrations on a hot strip mill cooling system are demonstrated in Section VI. Finally, the concluding remarks are presented in Section VII.

II. Preliminaries and Problem Statement

Notations: $\mathbb{R}^n$ denotes n-dimensional Euclidean space, and the norm is denoted as $|\cdot|_2$. $\mathcal{L}^2([0,L]) \triangleq \mathcal{L}^2((0,L);\mathbb{R})$ is a real Hilbert space of square integrable functions $\omega(x) : [0,L] \to \mathbb{R}$, and the spatial $\mathcal{L}^2$ norm is defined by $||\omega(\cdot)||_2 \triangleq \sqrt{\int_0^L \omega^2(x)\mathrm{d}x}$. Given a natural number $\bar{l}$, $\mathcal{H}^{\bar{l}}(0,1) \triangleq \mathcal{W}^{\bar{l},2}((0,1);\mathbb{R})$ is a real Sobolev space of absolutely continuous functions $\bar{\omega}(x) : (0,1) \to \mathbb{R}$ with square integrable derivatives $\mathrm{d}^i\bar{\omega}(x)/\mathrm{d}x^i$ up to the order $\bar{l} \geq 1$ and with the norm $||\bar{\omega}(\cdot)||_{\mathcal{H}^{\bar{l}}} \triangleq \sqrt{\int_0^1 \sum_{i=0}^{\bar{l}} (\frac{\mathrm{d}^i\bar{\omega}(x)}{\mathrm{d}x^i})^2\mathrm{d}x}$. For any functions $\omega(\cdot) \in \mathcal{H}^1(0,1)$, the spatial $\mathcal{L}^\infty$ norm is defined as $||\omega(\cdot)||_\infty \triangleq \max_{x\in[0,1]} |\omega(x)|$. $T_t \triangleq \partial T/\partial t$, $T_x \triangleq \partial T/\partial x$, $T_{xx} \triangleq \partial^2 T/\partial x^2$.

A. Process Description

We consider the distributed parameter processes that can be described by the following PDE:

$$T_t(x,t) = T_{xx}(x,t) + d(x,t) + f(x,t) \tag{1a}$$
$$T_x(0,t) = \eta_1 T(0,t) \tag{1b}$$
$$T_x(1,t) = -\eta_2 T(1,t) \tag{1c}$$
$$T(x,0) = T_0(x) \tag{1d}$$
$$\boldsymbol{y}(t) = \int_0^1 \boldsymbol{c}(x)T(x,t)\mathrm{d}x \tag{1e}$$

where $T(\cdot,t) \in \mathcal{L}^2([0,1])$ denotes the state variable, $x \in [0,1]$ denotes the space variable and $t \in [0,\infty)$ is the time variable, $d(x,t)$ is the *unknown* disturbance (including process noise and model uncertainty) in the system, $f(x,t)$ is the *unknown* fault, $\boldsymbol{y}(t) \triangleq [y_1(t) \quad y_2(t) \quad \cdots \quad y_n(t)]^T \in \mathbb{R}^n$ denotes the n-dimensional sensor output, and $\boldsymbol{c}(x) \triangleq [c_1(x) \quad c_2(x) \quad \cdots \quad c_n(x)]^T \in \mathbb{R}^n$ characterizes the measurement scheme. Without loss of generality, the most frequently used *pointwise measurement* [34], [35] is selected with

$$c_i(x) = \delta(x - \bar{x}_i), \quad i \in \mathcal{N} \triangleq \{1, 2, \ldots, n\}$$

corresponding to the pointwise measurement located on $\bar{x}_i$, $i \in \mathcal{N}$ in the spatial domain $(0,1)$ and $\delta(\cdot)$ denotes the Dirac delta function.

Assumption 1: The distributed disturbance $d(x,t)$ satisfies that

$$||d(\cdot,t)||_2 \leq \bar{d} < \infty$$

where $\bar{d} > 0$ is a *known* constant.

Remark 1: It is worth noting that both fault $f(x,t)$ and disturbance $d(x,t)$ exist in the system. It is a common setting in the literature that the fault and disturbance exist in both ODE systems [20] and PDE systems [13], [30], [36]. In fact, the disturbance (unknown input) $d(x,t)$ consists of model uncertainty and process noises. As for the term $f(x,t)$, it represents all possible faults and will be 0 in the fault-free case. This setting is essential for robust fault detection; otherwise, a false alarm may arise.

B. Problem Statement

The problem considered can be formulated as follows:

Use pointwise measurement $\boldsymbol{y}(t)$ to design an FDF and generate the corresponding residual signal for *reliable fault detection* for distributed parameter processes that subject to the state-space description of the form in (1a)–(1e).

III. Methodology Framework

A. Motivation

The core of model-based fault diagnosis methods for ODE systems lies in the construction of the analytical redundancy [20], which can be used for the residual generation. Bearing this in mind, we intend to construct an FDF in a mimic way.

Note that for ODE systems, both the state variable and output are of finite dimension. However, for systems described by (1), the state variable $T(x,t)$ is of *infinite dimension* while the output $\boldsymbol{y}(t)$ is of finite dimension. One major challenge in designing the FDF is how to map the finite-dimensional output to the infinite-dimensional state variable to complete the so-called *output injection* procedure.

Despite the fact that the backstepping-based boundary observer design shows its superiority in simple design procedures (see [5], [13], [32], [33], and [37] for reference), how to expand it to cover in-domain (pointwise and piecewise [34]) measurement requires more research efforts. This becomes extremely essential for fault detection of distributed parameter processes since in-domain measurement increases the redundancy of the FDF.

To this end, we intend to investigate the FDF design for distributed parameter processes covering both the boundary measurement, pointwise measurement, and piecewise

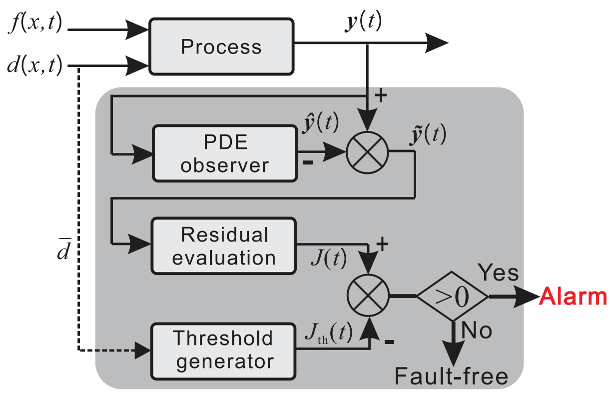

Fig. 1. Methodology framework.

measurement cases motivated by the *unified* Lyapunov-based compensator design [38]. To facilitate the FDF design, some results in [38] are further extended from the spatial $\mathcal{L}^2$ norm to spatial $\mathcal{L}^\infty$ norm.

B. Proposed Framework

Motivated by the above considerations, a framework that consists of an FDF and the corresponding residual evaluation and threshold computation procedures is introduced in Fig. 1 as follows.

IV. Spatial Domain Decomposition-Based PDE Observer Design & Analysis

Motivated by the spatial-domain decomposition technique introduced in [34] and [38], the following PDE observer is initiated for system (1a)–(1e):

$$\hat{T}_t(x,t) = \hat{T}_{xx}(x,t) + \boldsymbol{g}^T(x)\boldsymbol{L}(\boldsymbol{y}(t) - \hat{\boldsymbol{y}}(t)) \tag{2a}$$
$$\hat{T}_x(0,t) = \eta_1\hat{T}(0,t) \tag{2b}$$
$$\hat{T}_x(1,t) = -\eta_2\hat{T}(1,t) \tag{2c}$$
$$\hat{\boldsymbol{y}}(t) = \int_0^1 \boldsymbol{c}(x)\hat{T}(x,t)\mathrm{d}x \tag{2d}$$

where $\boldsymbol{g}(x) \triangleq [g_1(x) \quad g_2(x) \quad \cdots \quad g_n(x)]^T$ and the elements are defined as

$$g_i(x) \triangleq \begin{cases} 1, & x \in [x_i, x_{i+1}] \\ 0, & x \notin [x_i, x_{i+1}] \end{cases} \quad i \in \mathcal{N} \tag{3}$$

such that $\bar{x}_i \in (x_i, x_{i+1}), i \in \mathcal{N}, 0 = x_1 < x_2 < \cdots < x_n < x_{n+1} = 1$, and $\boldsymbol{L} \triangleq \operatorname{diag}\{l_1, l_2, \ldots, l_n\}$ is the gain matrix for the observer. This is the main idea of the spatial-domain decomposition approach [34], [39], as illustrated in Fig. 2.

Introducing the state error variable $e(x,t) \triangleq T(x,t) - \hat{T}(x,t)$, and the output error variable $\tilde{\boldsymbol{y}}(t) \triangleq \boldsymbol{y}(t) - \hat{\boldsymbol{y}}(t)$, the following error system is obtained:

$$\begin{aligned} e_t(x,t) &= e_{xx}(x,t) + f(x,t) + d(x,t) \\ &\quad - \boldsymbol{g}^T(x)\boldsymbol{L}\int_0^1 \boldsymbol{c}(x)e(x,t)\mathrm{d}x \end{aligned} \tag{4a}$$
$$e_x(0,t) = \eta_1 e(0,t) \tag{4b}$$
$$e_x(1,t) = -\eta_2 e(1,t) \tag{4c}$$

by combining (1) with (2).

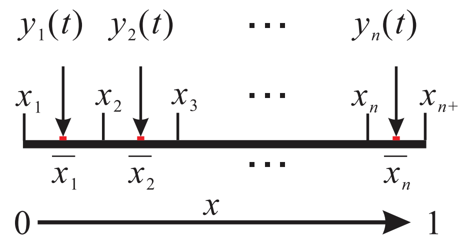

Fig. 2. Illustration of the spatial decomposition approach with pointwise measurement.

Lemma 1 [38]: Given a scalar function $z \in \mathcal{H}^1(0,1)$, the following inequality holds:

$$\int_0^1 (z(y) - z(\bar{x}))^2\mathrm{d}s \le 4\phi\pi^{-2}\int_0^1 (\mathrm{d}z(y)/\mathrm{d}y)^2\mathrm{d}y$$

where $\bar{x} \in [0,1]$, $\phi \triangleq \max\{\bar{x}^2, (1-\bar{x})^2\}$.

Lemma 2 [40]: Given regular real functions $V(t)$ and $h(t)$

$$\dot{V}(t) \le -\beta V(t) + h(t) \quad \forall t \ge 0$$

implies that

$$V(t) \le e^{-\alpha t}V(0) + \int_0^t e^{-\beta(t-\upsilon)}h(\upsilon)\mathrm{d}\upsilon \quad \forall t \ge 0$$

for any finite positive constant α.

Lemma 3 (Agmon's Inequality [32]): Given a scalar function $z \in \mathcal{H}^1(0,1)$, the following inequalities hold:

$$\begin{aligned} ||z(\cdot,t)||_\infty^2 &\le z^2(0,t) + 2||z(\cdot,t)||_2||z_y(\cdot,t)||_2, \\ ||z(\cdot,t)||_\infty^2 &\le z^2(1,t) + 2||z(\cdot,t)||_2||z_y(\cdot,t)||_2. \end{aligned}$$

Theorem 1 (Fault Detectability): For positive constant γ, if there exist positive scalars p, $q \in (0, (8/\pi^2))$ and $\bar{l}_i, i \in \mathcal{N}$ such that the following LMIs can be satisfied:

$$\boldsymbol{\Psi}_i + \frac{p\eta_1 q}{2}\boldsymbol{I} \le 0, i \in \mathcal{N} \tag{5}$$

where

$$\boldsymbol{\Psi}_i \triangleq \begin{bmatrix} -\frac{p\pi^2}{4\phi_i} & \star & \star & \star \\ \left(\frac{p\pi^2}{4\phi_i} - \frac{\bar{l}_i}{2}\right) & -\frac{p\pi^2}{4\phi_i} & \star & \star \\ 0 & \frac{\bar{l}_i}{2} & -p & \star \\ \frac{p}{2} & 0 & -\frac{p}{2} & -\gamma^2 \end{bmatrix}, \quad i \in \mathcal{N}$$

and $\phi_i \triangleq \max\{(\bar{x}_i - x_i)^2, (x_{i+1} - \bar{x}_i)^2\}$, then $e(x,t)$ is uniformly ultimately bounded (UUB) in the sense of $||\cdot||_\infty$ with ultimate bound $\bar{e}$ where

$$\bar{e} \triangleq \sqrt{\frac{2}{p\min\{\eta_1, 1\}\bar{\rho}}}\gamma\bar{d} \tag{6}$$

with

$$\bar{\rho} \triangleq \min\left\{\eta_1 q, 2 - \frac{q\pi^2}{4}\right\}. \tag{7}$$

The elements l_i of the observer gain matrix can be calculated according to

$$l_i = p^{-1}\bar{l}_i, i \in \mathcal{N}. \tag{8}$$

Proof: Consider the following Lyapunov function:

$$V(t) \triangleq V_1(t) + V_2(t) \tag{9}$$

where

$$\begin{aligned} V_1(t) &\triangleq \frac{p}{2}\int_0^1 \left(e^2(x,t) + e_x^2(x,t)\right)\mathrm{d}x \\ V_2(t) &\triangleq \frac{p\eta_1}{2}e^2(0,t) + \frac{p\eta_2}{2}e^2(1,t). \end{aligned} \tag{10}$$

The time derivative of $V_1(t)$ can be calculated as

$$\begin{aligned} \dot{V}_1(t) = &\int_0^1 pe(x,t)e_t(x,t)\mathrm{d}x \\ &+ \int_0^1 pe_x(x,t)e_{xt}(x,t)\mathrm{d}x. \end{aligned} \tag{11}$$

Set

$$\bar{l}_i = pl_i, i \in \mathcal{N}.$$

Using integration by parts, one gets

$$\begin{aligned} \int_0^1 pe(x,t)e_t(x,t)\mathrm{d}x = &\underbrace{\int_0^1 pe(x,t)e_{xx}(x,t)\mathrm{d}x}_{\text{Intergration by parts+(4b)−(4c)}} \\ &- \int_0^1 pe(x,t)\boldsymbol{g}^T(x)\boldsymbol{L}\mathrm{d}x\int_0^1 \boldsymbol{c}(x)e(x,t)\mathrm{d}x \\ &+ \int_0^1 pe(x,t)d(x,t)\mathrm{d}x \\ = &-p\eta_2 e^2(1,t) - p\eta_1 e^2(0,t) \\ &- \int_0^1 pe_x^2(x,t)\mathrm{d}x \\ &- \sum_{i=1}^n \int_{x_i}^{x_{i+1}} \bar{l}_i e(x,t)e(\bar{x}_i,t)\mathrm{d}x \\ &+ \int_0^1 pe(x,t)d(x,t)\mathrm{d}x \end{aligned} \tag{12}$$

by combining with (4a) and the boundary conditions in (4b) and (4c).

Moreover, the last term in the RHS of (11) is further formulated as

$$\begin{aligned} &\underbrace{\int_0^1 pe_x(x,t)e_{xt}(x,t)\mathrm{d}x}_{\text{Intergration by parts+(4b)−(4c)}} \\ &= -p\eta_2 e(1,t)e_t(1,t) - p\eta_1 e(0,t)e_t(0,t) \\ &\quad - \int_0^1 pe_{xx}(x,t)e_t(x,t)\mathrm{d}x \\ &= -p\eta_2 e(1,t)e_t(1,t) - p\eta_1 e(0,t)e_t(0,t) \\ &\quad - \int_0^1 pe_{xx}^2(x,t)\mathrm{d}x + \sum_{i=1}^n \int_{x_i}^{x_{i+1}} \bar{l}_i e_{xx}(x,t)e(\bar{x}_i,t)\mathrm{d}x \\ &\quad - \int_0^1 pe_{xx}(x,t)d(x,t)\mathrm{d}x \end{aligned} \tag{13}$$

considering (4a) and the boundary conditions in (4b) and (4c).

Combining (12) with (13), it can be obtained that

$$\begin{aligned} \dot{V}_1(t) = &-p\eta_2 e^2(1,t) - p\eta_1 e^2(0,t) - p\eta_2 e(1,t)e_t(1,t) \\ &- p\eta_1 e(0,t)e_t(0,t) - \int_0^1 pe_x^2(x,t)\mathrm{d}x \\ &- \int_0^1 pe_{xx}^2(x,t)\mathrm{d}x - \sum_{i=1}^n \int_{x_i}^{x_{i+1}} \bar{l}_i e(x,t)e(\bar{x}_i,t)\mathrm{d}x \\ &+ \sum_{i=1}^n \int_{x_i}^{x_{i+1}} \bar{l}_i e_{xx}(x,t)e(\bar{x}_i,t)\mathrm{d}x \\ &+ \int_0^1 pe(x,t)d(x,t)\mathrm{d}x - \int_0^1 pe_{xx}(x,t)d(x,t)\mathrm{d}x. \end{aligned} \tag{14}$$

Moreover, it can be calculated that

$$\dot{V}_2(t) = p\eta_1 e(0,t)e_t(0,t) + p\eta_2 e(1,t)e_t(1,t). \tag{15}$$

Combining (14) and (15), it can be derived that

$$\begin{aligned} \dot{V}(t) = &-p\eta_2 e^2(1,t) - p\eta_1 e^2(0,t) - \int_0^1 pe_x^2(x,t)\mathrm{d}x \\ &- \int_0^1 pe_{xx}^2(x,t)\mathrm{d}x - \sum_{i=1}^n \int_{x_i}^{x_{i+1}} \bar{l}_i e(x,t)e(\bar{x}_i,t)\mathrm{d}x \\ &+ \sum_{i=1}^n \int_{x_i}^{x_{i+1}} \bar{l}_i e_{xx}(x,t)e(\bar{x}_i,t)\mathrm{d}x \\ &+ \int_0^1 pe(x,t)d(x,t)\mathrm{d}x - \int_0^1 pe_{xx}(x,t)d(x,t)\mathrm{d}x. \end{aligned} \tag{16}$$

Using Lemma 1 for each interval $[x_i, x_{i+1}]$, $i \in \mathcal{N}$, it can be derived that

$$\int_{x_i}^{x_{i+1}} e_x^2(x,t)\mathrm{d}x \geq \frac{\pi^2}{4\phi_i}\int_{x_i}^{x_{i+1}} (e(x,t) - e(\bar{x}_i,t))^2\mathrm{d}x. \tag{17}$$

Substituting (17) into (16) and recalling that $0 = x_1 < x_2 < \cdots < x_n < x_{n+1} = 1$ and $\eta_1 > 0$, $\eta_2 > 0$, we have that

$$\begin{aligned} \dot{V}(t) \leq &-p\eta_2 e^2(1,t) - p\eta_1 e^2(0,t) - \sum_{i=1}^n \int_{x_i}^{x_{i+1}} \frac{p\pi^2}{4\phi_i}e^2(x,t)\mathrm{d}x \\ &- \sum_{i=1}^n \int_{x_i}^{x_{i+1}} \frac{p\pi^2}{4\phi_i}e^2(\bar{x}_i,t)\mathrm{d}x - \sum_{i=1}^n \int_{x_i}^{x_{i+1}} pe_{xx}^2(x,t)\mathrm{d}x \\ &+ \sum_{i=1}^n \int_{x_i}^{x_{i+1}} \left(\frac{p\pi^2}{2\phi_i} - \bar{l}_i\right)e(x,t)e(\bar{x}_i,t)\mathrm{d}x \\ &+ \sum_{i=1}^n \int_{x_i}^{x_{i+1}} \bar{l}_i e_{xx}(x,t)e(\bar{x}_i,t)\mathrm{d}x \\ &+ \sum_{i=1}^n \int_{x_i}^{x_{i+1}} pe(x,t)d(x,t)\mathrm{d}x \\ &- \sum_{i=1}^n \int_{x_i}^{x_{i+1}} pe_{xx}(x,t)d(x,t)\mathrm{d}x \\ = &\sum_{i=1}^n \int_{x_i}^{x_{i+1}} \boldsymbol{\xi}_i^T(x,t)\boldsymbol{\Psi}_i\boldsymbol{\xi}_i(x,t)\mathrm{d}x - p\eta_2 e^2(1,t) \\ &- p\eta_1 e^2(0,t) + \gamma^2||d(\cdot,t)||_2^2 \end{aligned} \tag{18}$$

where

$$\boldsymbol{\xi}_i(x,t) \triangleq [e(x,t) \quad e(\bar{x}_i,t) \quad e_{xx}(x,t) \quad d(x,t)]^T.$$

By substituting (5) into (18) and considering Assumption 1, it can be obtained that

$$\begin{aligned}\dot{V}(t) &\le -\frac{p\eta_1 q}{2}\sum_{i=1}^{n}\int_{x_i}^{x_{i+1}} \boldsymbol{\xi}_i^T(x,t)\boldsymbol{\Psi}_i\boldsymbol{\xi}_i(x,t)\mathrm{d}x \\ &\quad - p\eta_2 e^2(1,t) - p\eta_1 e^2(0,t) + \gamma^2\bar{d}^2 \\ &\le -\frac{p\eta_1 q}{2}\left(||e(\cdot,t)||_2^2 + ||e_{xx}(\cdot,t)||_2^2\right) - p\eta_2 e^2(1,t) \\ &\quad - p\eta_1 e^2(0,t) + \gamma^2\bar{d}^2 \\ &\le -\Bigg(\eta_1 q\frac{p}{2}||e(\cdot,t)||_2^2 + \frac{\pi^2\eta_1 q}{4}\frac{p}{2}||e_x(\cdot,t)||_2^2 \\ &\quad + 2\frac{p\eta_2}{2}e^2(1,t) + \left(2 - \frac{q\pi^2}{4}\right)\frac{p\eta_1}{2}e^2(0,t)\Bigg) + \gamma^2\bar{d}^2 \\ &\le -\bar{\rho}V(t) + \gamma^2\bar{d}^2 \end{aligned} \tag{19}$$

by applying Lemma 1 and recalling the definition of $\bar{\rho}$ in (7).

Hence, one gets

$$V(t) \le V(0)\exp(-\bar{\rho}t) + \frac{\gamma^2\bar{d}^2}{\bar{\rho}} \tag{20}$$

by Lemma 2.

Recalling Lemma 3 and Young's inequality [32], we get

$$\begin{aligned}||e(\cdot,t)||_\infty^2 &\le e^2(0,t) + 2||e(\cdot,t)||_2||e_x(\cdot,t)||_2 \\ &\le e^2(0,t) + ||e(\cdot,t)||_2^2 + ||e_x(\cdot,t)||_2^2 \\ &\le e_B^2(t) \triangleq \frac{2V(0)}{p\min\{\eta_1,1\}}\exp(-\bar{\rho}t) + \bar{e}^2 \end{aligned} \tag{21}$$

using (20).

Recalling Assumption 1, one gets that $0 < \bar{e} < \infty$. Hence, $e(x,t)$ satisfies the UUB condition in the sense of $||\cdot||_\infty$ while the ultimate bound is $\bar{e}$. ■

Remark 2: Note that when using the Poincaré–Wirtinger inequality's variants and Agmon's inequality for deriving (19) and (21), respectively, $e(0,t)$ is considered in both inequalities. One can consider replacing it with $e(1,t)$ instead, and LMIs in (5) change to

$$\boldsymbol{\Psi}_i + \frac{p\eta_2 q}{2}\boldsymbol{I} \le 0, i \in \mathcal{N}$$

corresponding under this condition. Moreover, one can get an ultimate bound following the same procedures. The details are not discussed due to triviality.

Remark 3: The proposed spatial domain decomposition approach contains the boundary measurement at $x = 0$ or $x = 1$ if $\bar{x}_1 = 0$ for $\bar{x}_{n+1} = 1$. Moreover, the results can be easily expanded to the piecewise measurement case, as shown in [38]. Furthermore, the results are also applicable for the homogeneous Dirichlet boundary conditions, homogeneous Neumann boundary conditions, mixed homogeneous Neumann–Dirichlet boundary conditions, and mixed homogeneous Dirichlet-Neumann boundary conditions. These extensions are trivial exercises and are not discussed.

V. FDF Design & Analysis

For the fault detection purpose, the following residual signal $\boldsymbol{r}(t)$ is selected intuitively:

$$\boldsymbol{r}(t) = \tilde{\boldsymbol{y}}(t). \tag{22}$$

Then, we show the *lumped* evaluation scheme and the threshold as follows:

$$J(t) = \int_t^{t+\Delta} |\boldsymbol{r}(\tau)|_2^2 \mathrm{d}\tau \tag{23a}$$

$$J_{\text{th}}(t) = \sup_{f(x,t)=0} J(t) \tag{23b}$$

where $\Delta > 0$ is the length of the evaluation time window.

Remark 4: There are several residual evaluation functions that are widely used in fault detection, such as the peak value, the average value, the root-mean-square (RMS) value, and the $\mathcal{L}_2$ norm [20]. The RMS value and $\mathcal{L}_2$ norm are related and are designed to reduce the false alarm rate (FAR) at the cost of fault detectability. It is worth noticing that $(\int_t^{t+T} |\boldsymbol{r}(\tau)|^2\mathrm{d}\tau)^{1/2}$ is a general form of the $\mathcal{L}_2$ norm [20], [41] of the signal $\boldsymbol{r}(t)$, which measures the energy of a signal over a time interval $[t, t+T]$. Since evaluation over the whole time domain is usually unrealistic, introducing an evaluation window is a practical modification [20]. This kind of evaluation function was widely used in the literature discussing FD issues of dynamic systems (see [42] and [43]).

Hence the following decision logic will guarantee reliable detection performance:

$$\begin{cases} J(t) > J_{\text{th}}(t) \Longrightarrow \text{ faulty at time } t \\ \text{Otherwise} \Longrightarrow \text{ fault-free at time } t. \end{cases} \tag{24}$$

Theorem 2: (Fault Detection Threshold Calculation) Under the lumped residual evaluation function in (23), if the conditions in Theorem 1 are satisfied, the time-varying detection threshold $J_{\text{th}}(t)$ for fault detection can be computed as

$$J_{\text{th}}(t) = \int_t^{t+\Delta} n e_B^2(\tau)\mathrm{d}\tau. \tag{25}$$

Proof: The proof is based on (21) and the property of $||\cdot||_\infty$. It is omitted due to triviality.

Remark 5: It is worth noting that the threshold $J_{\text{th}}(t)$ is designed to be time varying rather than a constant that is frequently used [29], [33]. The intuitive idea is that the initial error $e_0(x)$ contributes to $V(0)$ and the time-varying term in (25) is decreasing exponentially with time, if only the ultimate bound $\bar{e}$ is considered in the threshold setting, one inevitable outcome is the false alarm in the initial transition stage [29]. To decrease the FAR, we add the compensate time-varying term in the threshold.

VI. Illustrative Example

A. System Description

Consider the following thermal model of a hot strip mill [24], [44]–[46] under the *fault-free* and *disturbance-free* conditions:

$$\rho c\bar{T}_\tau(\xi,\tau) = k\bar{T}_{\xi\xi}(\xi,\tau) \tag{26a}$$

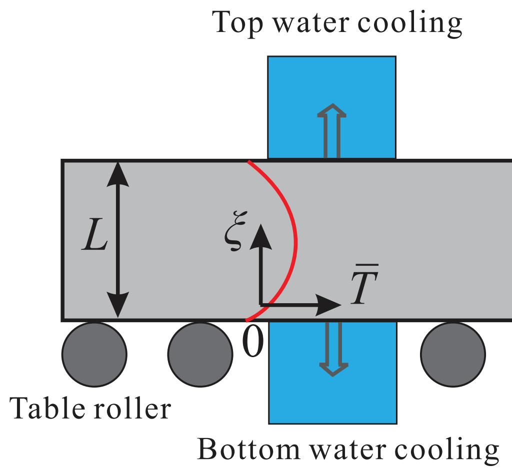

Fig. 3. Hot strip mill cooling system.

TABLE I
PROCESS PARAMETER SETTING

	Definition (Unit)	Value
L	Thickness ([m])	0.01
ρ	Density ([Kg/m^3])	7850
k	Average thermal conductivity ([W/m $^\circ$ C])	28
c	Average specific heat ([J/Kg $^\circ$ C])	932
h	Heat transfer coefficients([W/m^2 $^\circ$ C])	2000
T_w	Temperature of the cooling water ([$^\circ$ C])	30

$$\bar{T}_\xi(0,\tau) = \frac{h}{k}\big(\bar{T}(0,\tau) - T_w\big) \tag{26b}$$
$$\bar{T}_\xi(L,\tau) = -\frac{h}{k}\big(\bar{T}(L,\tau) - T_w\big) \tag{26c}$$
$$\bar{T}(\xi,0) = \bar{T}_0(\xi) \tag{26d}$$

where $\bar{T}(\xi,\tau) \in \mathcal{L}^2([0,L])$ denotes the temperature distribution along the thickness direction and L is the thickness of the strip, $\xi \in [0,L]$ is the space variable, $\tau \in [0,\infty)$ denotes the time, ρ is the density, k denotes the average value of thermal conductivity while c is the average value of specific heat, h denotes the heat transfer coefficient, and T_w denotes the temperature of water. Fig. 3 presents the layout of a strip on the ROT.

To facilitate the analysis, considering the disturbance and fault existing in the process and applying the scaling transformation [32], [44]

$$x = \frac{\xi}{L}$$
$$t = \frac{k\tau}{\rho c L^2}$$
$$T = \frac{\bar{T} - T_w}{\bar{T}_0 - T_w}$$

to system (26) leads to the following normalized equation:

$$\begin{aligned}
T_t(x,t) &= T_{xx}(x,t) + d(x,t) + f(x,t)\\
T_x(0,t) &= \eta T(0,t)\\
T_x(1,t) &= -\eta T(1,t)\\
T(x,0) &= T_0(x) = 1\\
y(t) &= T(0,t)
\end{aligned}$$

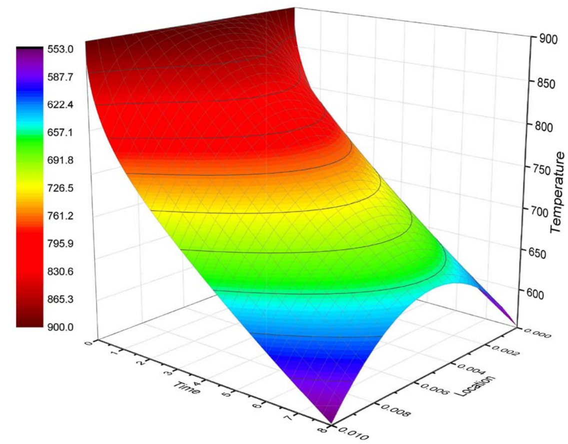

Fig. 4. Temperature distribution profile $\bar{T}(\xi,\tau)$ under normal operating condition.

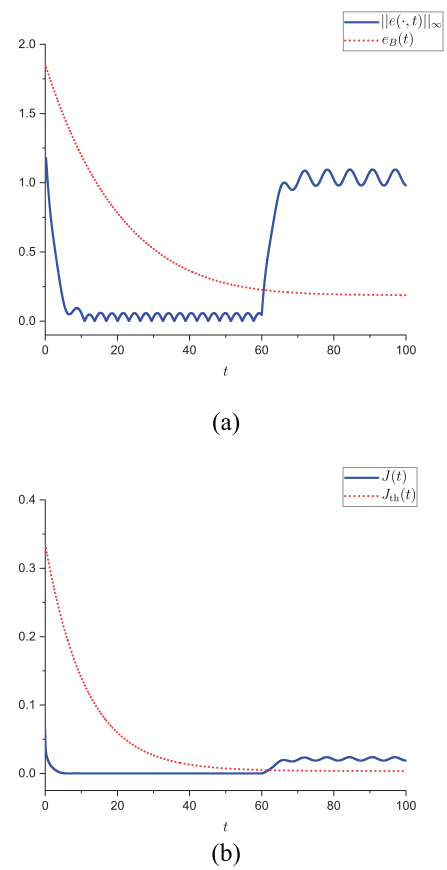

Fig. 5. Simulation results with abrupt fault. (a) Trajectory of $||e(\cdot,t)||_\infty$ and $e_B(t)$. (b) Trajectory of $J(t)$ and $J_{\rm th}(t)$.

where $\eta \triangleq \frac{hL}{k} > 0$. For practical consideration, the *boundary* measurement $T(0,t)$ on the bottom of the strip is used for fault detection.

B. Parameter Setting

Typically, the strip's temperature decreases from nearly 900 °C to 650 °C [44]; hence, the initial condition in (26d) is selected as $\bar{T}_0(\xi) = 900$ without loss of generality. Moreover, as illustrated in [44] and [47], the parameters used in the

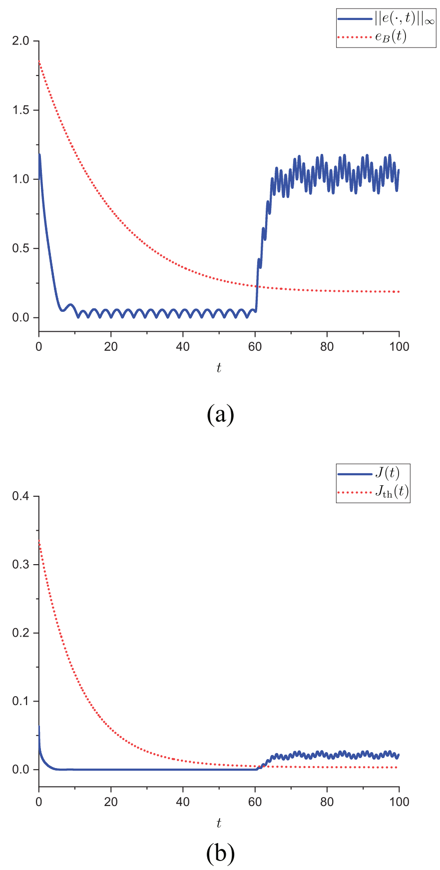

Fig. 6. Simulation results with periodic fault. (a) Trajectory of $||e(\cdot,t)||_\infty$ and $e_B(t)$. (b) Trajectory of $J(t)$ and $J_{\text{th}}(t)$.

simulation along with their practical values are summarized in Table I.

C. Simulation Results

The simulation result of system (26) under normal operating condition is presented in Fig. 4. The following disturbance is considered:

$$d(x,t) = 0.05 \exp\left(-0.5(x-0.5)^2\right)\sin(t).$$

Furthermore, the following fault is injected:

$$f(x,t) = b_f(x)f(t)$$

where

$$b_f(x) = H(x-0.5) - H(x-0.75)$$

is the shape function of the fault with $H(\cdot)$ denoting the standard Heaviside function. Two kinds of faults are considered

$$\text{Abrupt fault:} f(t) = \begin{cases} 0, & t \in [0,60) \\ 1, & t \in [60,\infty) \end{cases}$$

$$\text{Periodic fault:} f(t) = \begin{cases} 0, & t \in [0,60) \\ 1+\sin(5t), & t \in [60,\infty). \end{cases}$$

Selecting the evaluation time window $\Delta = 0.1$, the simulation results of both abnormal fault and periodic fault are presented in Figs. 5 and 6, respectively. One can find that the fault detection time $t = 60$ can be well detected for both faults. Moreover, results in Figs. 5(a) and 6(a) show that $||e(\cdot,t)||_\infty$ is UUB in the fault-free scenario, which demonstrated the correctness of Theorem 1.

VII. Conclusion

In this article, a unified framework for fault detection consisting of both the boundary and in-domain sensors was proposed without modal approximation or interpolation. An FDF based on the PDE observer was developed, which is motivated by the FDF design for LPSs. Rigorous theoretic analysis was presented to guarantee the reliability of the proposed detection scheme. Motivated by the fact that for real industrial processes, the system model may not be completely known, hence it would be interesting to further investigate the fault detection problem of these processes with partially known or even unknown system parameters in the future.

References

[1] N. H. El-Farra and S. Ghantasala, "Actuator fault isolation and reconfiguration in transport-reaction processes," *AIChE J.*, vol. 53, no. 6, pp. 1518–1537, 2007.
[2] H. Deng, H.-X. Li, and G. Chen, "Spectral-approximation-based intelligent modeling for distributed thermal processes," *IEEE Trans. Control Syst. Technol.*, vol. 13, no. 5, pp. 686–700, Sep. 2005.
[3] L.-Q. Chen, H.-X. Li, and H.-D. Yang, "Dimension embedded basis function for spatiotemporal modeling of distributed parameter system," *IEEE Trans. Ind. Informat.*, vol. 16, no. 9, pp. 5846–5854, Sep. 2020.
[4] L. Chen, H.-X. Li, and H.-D. Yang, "Spatiotemporal modeling for distributed parameter system under sparse sensing," *Ind. Eng. Chem. Res.*, vol. 59, pp. 16321–16329, Aug. 2020.
[5] S. Dey, H. E. Perez, and S. J. Moura, "Model-based battery thermal fault diagnostics: Algorithms, analysis, and experiments," *IEEE Trans. Control Syst. Technol.*, vol. 27, no. 2, pp. 576–587, Mar. 2019.
[6] B.-C. Wang, H.-X. Li, and H.-D. Yang, "Spatial correlation-based incremental learning for spatiotemporal modeling of battery thermal process," *IEEE Trans. Ind. Electron.*, vol. 67, no. 4, pp. 2885–2893, Apr. 2020.
[7] X.-B. Meng, H.-X. Li, and H.-D. Yang, "Evolutionary design of spatio–temporal learning model for thermal distribution in lithium-ion batteries," *IEEE Trans. Ind. Informat.*, vol. 15, no. 5, pp. 2838–2848, May 2019.
[8] H.-X. Li and C. Qi, "Modeling of distributed parameter systems for applications—A synthesized review from time–space separation," *J. Process Control*, vol. 20, no. 8, pp. 891–901, 2010.
[9] Z. Wang, H.-X. Li, and C. Chen, "Reinforcement learning-based optimal sensor placement for spatiotemporal modeling," *IEEE Trans. Cybern.*, vol. 50, no. 6, pp. 2861–2871, Jun. 2020.
[10] S.-H. Tsai, J.-W. Wang, E.-S. Song, and H.-K. Lam, "Robust $\mathcal{H}_\infty$ control for nonlinear hyperbolic PDE systems based on the polynomial fuzzy model," *IEEE Trans. Cybern.*, early access, Oct. 9, 2019, doi: 10.1109/TCYB.2019.2942685.
[11] J.-W. Wang, "Dynamic boundary fuzzy control design of semilinear parabolic PDE systems with spatially noncollocated discrete observation," *IEEE Trans. Cybern.*, vol. 49, no. 8, pp. 3041–3051, Aug. 2019.
[12] J.-W. Wang and H.-N. Wu, "Design of suboptimal local piecewise fuzzy controller with multiple constraints for quasi-linear spatiotemporal dynamic systems," *IEEE Trans. Cybern.*, early access, Jul. 4, 2019, doi: 10.1109/TCYB.2019.2923461.
[13] S. Dey, H. E. Perez, and S. J. Moura, "Robust fault detection of a class of uncertain linear parabolic PDEs," *Automatica*, vol. 107, pp. 502–510, Sep. 2019.
[14] N. H. El-Farra, "Integrated fault detection and fault-tolerant control architectures for distributed processes," *Ind. Eng. Chem. Res.*, vol. 45, no. 25, pp. 8338–8351, 2006.
[15] Z. Liu, J. Liu, and W. He, "Modeling and vibration control of a flexible aerial refueling hose with variable lengths and input constraint," *Automatica*, vol. 77, pp. 302–310, Mar. 2017.
[16] Z. Liu, X. He, Z. Zhao, C. K. Ahn, and H.-X. Li, "Vibration control for spatial aerial refueling hoses with bounded actuators," *IEEE Trans. Ind. Electron.*, early access, Apr. 9, 2020, doi: 10.1109/TIE.2020.2984442.

[17] Z.-P. Wang and H.-N. Wu, "Sampled-data fuzzy control with guaranteed cost for nonlinear parabolic PDE systems via static output feedback," *IEEE Trans. Fuzzy Syst.*, vol. 28, no. 10, pp. 2452–2465, Oct. 2020.

[18] Z.-P. Wang, H.-N. Wu, and T. Huang, "Sampled-data fuzzy control for nonlinear delayed distributed parameter systems," *IEEE Trans. Fuzzy Syst.*, early access, Jul. 28, 2020, doi: 10.1109/TFUZZ.2020.3012392.

[19] Z.-P. Wang, H.-N. Wu, and H.-X. Li, "Fuzzy control under spatially local averaged measurements for nonlinear distributed parameter systems with time-varying delay," *IEEE Trans. Cybern.*, early access, Jun. 4, 2019, doi: 10.1109/TCYB.2019.2916656.

[20] S. X. Ding, *Model-Based Fault Diagnosis Techniques: Design Schemes, Algorithms, And Tools*, 2nd ed. London, U.K.: Springer, 2013.

[21] C. Zhang, H. Yang, and B. Jiang, "Fault estimation and accommodation of fractional-order nonlinear, switched, and interconnected systems," *IEEE Trans. Cybern.*, early access, May 14, 2020, doi: 10.1109/TCYB.2020.2988731.

[22] H. Yang, C. Zhang, Z. An, and B. Jiang, "Exponential small-gain theorem and fault tolerant safe control of interconnected nonlinear systems," *Automatica*, vol. 115, May 2020, Art. no. 108866.

[23] S. X. Ding, *Data-Driven Design of Fault Diagnosis and Fault-Tolerant Control Systems*. London, U.K.: Springer, 2014.

[24] J. Dong, Q. Wang, M. Wang, and K. Peng, "Data-driven quality monitoring techniques for distributed parameter systems with application to hot-rolled strip laminar cooling process," *IEEE Access*, vol. 6, pp. 16646–16654, 2018.

[25] Y. Feng and H.-X. Li, "Detection and spatial identification of fault for parabolic distributed parameter systems," *IEEE Trans. Ind. Electron.*, vol. 66, no. 9, pp. 7300–7309, Sep. 2019.

[26] Y. Feng, H.-X. Li, and H.-D. Yang, "Abnormal source identification for parabolic distributed parameter systems," *IEEE Trans. Syst., Man, Cybern., Syst.*, early access, Dec. 19, 2019, doi: 10.1109/TSMC.2019.2956985.

[27] Y. Feng and H.-X. Li, "Dynamic spatial-independent-component-analysis-based abnormality localization for distributed parameter systems," *IEEE Trans. Ind. Informat.*, vol. 16, no. 5, pp. 2929–2936, May 2020.

[28] W. H. Ray, *Advanced Process Control*. New York, NY, USA: McGraw-Hill, 1981.

[29] S. Ghantasala and N. H. El-Farra, "Robust actuator fault isolation and management in constrained uncertain parabolic PDE systems," *Automatica*, vol. 45, no. 10, pp. 2368–2373, 2009.

[30] F. Fischer and J. Deutscher, "Flatness-based algebraic fault diagnosis for distributed-parameter systems," *Automatica*, vol. 117, Jul. 2020, Art. no. 108987.

[31] Y. Feng, Y. Wang, J.-W. Wang, and H.-X. Li, "Abnormal spatio-temporal source estimation for a linear unstable parabolic distributed parameter system: An adaptive PDE observer perspective," *J. Franklin Inst.*, vol. 358, no. 2, pp. 1656–1672, 2021.

[32] M. Krstić and A. Smyshlyaev, *Boundary Control of PDEs: A Course on Backstepping Designs*, vol. 16. Philadelphia, PA, USA: SIAM, 2008.

[33] J. Cai, H. Ferdowsi, and J. Sarangapani, "Model-based fault detection, estimation, and prediction for a class of linear distributed parameter systems," *Automatica*, vol. 66, pp. 122–131, Apr. 2016.

[34] J.-W. Wang, Y.-Q. Liu, Y.-Y. Hu, and C.-Y. Sun, "A spatial domain decomposition approach to distributed $\mathcal{H}_\infty$ observer design of a linear unstable parabolic distributed parameter system with spatially discrete sensors," *Int. J. Control*, vol. 90, no. 12, pp. 2772–2785, 2017.

[35] J.-W. Wang, Y.-Q. Liu, and C.-Y. Sun, "Pointwise exponential stabilization of a linear parabolic PDE system using non-collocated pointwise observation," *Automatica*, vol. 93, pp. 197–210, Jul. 2018.

[36] J. Deutscher, "Fault detection for linear distributed-parameter systems using finite-dimensional functional observers," *Int. J. Control*, vol. 89, no. 3, pp. 550–563, 2016.

[37] A. Smyshlyaev and M. Krstic, "Backstepping observers for a class of parabolic PDEs," *Syst. Control Lett.*, vol. 54, no. 7, pp. 613–625, 2005.

[38] J.-W. Wang, "A unified Lyapunov-based design for a dynamic compensator of linear parabolic MIMO PDEs," *Int. J. Control*, pp. 1–8, Oct. 2019.

[39] J.-W. Wang and J.-M. Wang, "Dynamic compensator design of linear parabolic MIMO PDEs in N-dimensional spatial domain," *IEEE Trans. Autom. Control*, early access, May 11, 2020, doi: 10.1109/TAC.2020.2994165.

[40] P. A. Ioannou and J. Sun, *Robust Adaptive Control*. Mineola, NY, USA: Dover, 2012.

[41] L. Li, S. X. Ding, K. Peng, J. Qiu, and Y. Yang, "Fuzzy fault detection filter design for nonlinear distributed parameter systems," *IEEE Access*, vol. 7, pp. 11105–11113, 2019.

[42] L. Li, S. X. Ding, J. Qiu, Y. Yang, and D. Xu, "Fuzzy observer-based fault detection design approach for nonlinear processes," *IEEE Trans. Syst., Man, Cybern., Syst.*, vol. 47, no. 8, pp. 1941–1952, Aug. 2017.

[43] L. Li and S. X. Ding, "Gap metric techniques and their application to fault detection performance analysis and fault isolation schemes," *Automatica*, vol. 118, Aug. 2020, Art. no. 109029. [Online]. Available: http://www.sciencedirect.com/science/article/pii/S0005109820302272

[44] R. K. Kumar, S. K. Sinha, and A. K. Lahiri, "Modeling of the cooling process on the runout table of a hot strip mill-a parallel approach," *IEEE Trans. Ind. Appl.*, vol. 33, no. 3, pp. 807–814, May/Jun. 1997.

[45] T. Hashimoto, Y. Yoshioka, and T. Ohtsuka, "Receding horizon control for hot strip mill cooling systems," *IEEE/ASME Trans. Mechatron.*, vol. 18, no. 3, pp. 998–1005, Jun. 2013.

[46] Z. Yang and X. Luo, "Parallel numerical calculation on GPU for the 3-dimensional mathematical model in the walking beam reheating furnace," *IEEE Access*, vol. 7, pp. 44583–44595, 2019.

[47] M. Prieto, L. Ruíz, and J. Menéndez, "Thermal performance of numerical model of hot strip mill runout table," *Ironmaking Steelmaking*, vol. 28, no. 6, pp. 474–480, 2001.

Yun Feng received the B.E. degree in automation and the M.S. degree in control theory and control engineering from the Department of Automation, Wuhan University, Wuhan, China, in 2014 and 2017, respectively, and the Ph.D. degree from the Department of Systems Engineering and Engineering Management, City University of Hong Kong, Hong Kong, in 2020.

In 2019, he was a visiting student with the Institute for Automatic Control and Complex Systems, University of Duisburg-Essen, Duisburg, Germany. He is currently a Postdoctoral Fellow with the College of Electrical and Information Engineering, Hunan University, Changsha, China, where he is also the National Engineering Laboratory for Robot Visual Perception and Control Technology. His current research interests include fault diagnosis of distributed parameter systems and unmanned systems.

Yaonan Wang received the B.S. degree in computer engineering from the East China University of Science and Technology, Fuzhou, China, in 1981, and the M.S. and Ph.D. degrees in control engineering from Hunan University, Changsha, China, in 1990 and 1994, respectively.

He was a Postdoctoral Research Fellow with the National University of Defense Technology, Changsha, from 1994 to 1995; a Senior Humboldt Fellow in Germany, from 1998 to 2000; and a Visiting Professor with the University of Bremen, Bremen, Germany, from 2001 to 2004. He has been a Professor with Hunan University since 1995. He has been a Member of Chinese Academy of Engineering, Beijing, China, since 2019. His current research interests include robot control, intelligent control and information processing, industrial process control, and image processing.

Bing-Chuan Wang received the B.E. degree in automation and the M.E. degree in control science and engineering from Central South University, Changsha, China, in 2013 and 2016, respectively, and the Ph.D. degree in system engineering and engineering management from the City University of Hong Kong, Hong Kong, in 2019.

He is an Assistant Professor with the School of Automation, Central South University. His current research interests include evolutionary computation, constrained optimization, and intelligent modeling.

Han-Xiong Li (Fellow, IEEE) received the B.E. degree in aerospace engineering from the National University of Defense Technology, Changsha, China, in 1982, the M.E. degree in electrical engineering from the Delft University of Technology, Delft, The Netherlands, in 1991, and the Ph.D. degree in electrical engineering from the University of Auckland, Auckland, New Zealand, in 1997.

He is a Professor with the Department of SEEM, City University of Hong Kong, Hong Kong. He has broad experience in both academia and industry. He has authored two books and about 20 patents, and published more than 200 SCI journal papers with H-index 48 (Web of science). His current research interests include process modeling and control, system intelligence, distributed parameter systems, and battery-management system.

Prof. Li was awarded the Distinguished Young Scholar (overseas) by the China National Science Foundation in 2004; the Chang Jiang Professorship by the Ministry of Education, China, in 2006; and the National Professorship in China Thousand Talents Program in 2010. He serves as an Associate Editor for IEEE TRANSACTIONS ON SYSTEMS, MAN, AND CYBERNETICS: SYSTEMS, and was an Associate Editor for the IEEE TRANSACTIONS ON CYBERNETICS from 2002 to 2016, and IEEE TRANSACTIONS ON INDUSTRIAL ELECTRONICS from 2009 to 2015. He serves as a Distinguished Expert for Hunan Government and China Federation of Returned Overseas Chinese.